

Decoupling method for dynamical mean-field theory calculations

Harald O. Jeschke* and Gabriel Kotliar†

Department of Physics & Astronomy, Rutgers University, 136 Frelinghuysen Road, Piscataway, New Jersey 08854-8019, USA

(Received 18 June 2004; revised manuscript received 25 August 2004; published 3 February 2005)

In this paper we explore the use of an equation of motion decoupling method as an impurity solver to be used in conjunction with the dynamical mean field self-consistency condition for the solution of lattice models. We benchmark the impurity solver against exact diagonalization, and apply the method to study the infinite U Hubbard model, the periodic Anderson model and the pd model. This simple and numerically efficient approach yields the spectra expected for strongly correlated materials, with a quasiparticle peak and a Hubbard band. It works in a large range of parameters, and therefore can be used for the exploration of real materials using the local density approximation and dynamical mean field theory.

DOI: 10.1103/PhysRevB.71.085103

PACS number(s): 71.27.+a, 71.30.+h

I. INTRODUCTION

Dynamical mean field theory (DMFT) was developed over the past 15 years into a powerful tool for the treatment of strongly correlated electron systems.¹⁻³ DMFT is based on the idea of mapping a complicated lattice model onto a single impurity model coupled to a noninteracting bath. It relies on the observation that the self-energy $\Sigma(\mathbf{k}, i\omega_n)$ becomes \mathbf{k} independent in infinite dimensions $d=\infty$,⁴ making a single site treatment with only temporal fluctuation exact in this limit. The DMFT approach derives its strength from the fact that it becomes exact in this nontrivial limit of $d=\infty$ or infinite lattice coordination. Perhaps surprisingly, DMFT proves to be a very good approximation even in $d=3$ dimensions. By replacing complicated models with a single impurity model, the DMFT equations can then be solved with one of the methods that have been developed to solve the Anderson impurity model.

The study of correlated materials has until a few years ago been conducted with two approaches that are very different in spirit. On the one hand, density functional theory (DFT) calculations in the local density approximation (LDA) have proven invaluable in the determination of the electronic structure of real materials but there are a number of strongly correlated materials where its predictions are even in qualitative disagreement with experiment. On the other hand, the study of model Hamiltonians has provided a qualitative understanding of many systems with strong correlations but due to its dependence on parameters this method lacks predictive power for new materials. The combination of the two approaches in the form of LDA+DMFT (Ref. 5) promises to deepen our understanding of strongly correlated materials as some initial successes demonstrate.⁶⁻⁸

A self-consistent LDA+DMFT calculation in a multiband situation requires the Anderson impurity model with arbitrary values for the bath to be solved many times (once for each point of the \mathbf{k} grid of the LDA calculation), thus making the impurity solver the bottleneck of the LDA+DMFT algorithm. Therefore it is important to find impurity solvers that are reliable and computationally cheap. Currently, the usual choices for solving the Anderson impurity model in the framework of LDA+DMFT are quantum Monte Carlo

(QMC),⁹ the noncrossing approximation (NCA),¹⁰ and the iterated perturbation theory (IPT).¹¹ Nevertheless, each of these methods has some drawbacks limiting its range of applicability. The QMC method is essentially exact, but becomes prohibitively expensive at low temperatures and for high interaction strength U . The NCA approximation, applied to the impurity model, exceeds the unitarity limit at low temperatures and leads to pathologies in the solutions of the DMFT equations. The IPT scheme, a method which was very successful at arbitrary filling in the one orbital situation, has encountered difficulties in its extension to the multiorbital case. This provides the motivation of this article to investigate the usefulness of a previously known decoupling scheme in the context of DMFT.

The method for the solution of the Anderson impurity model proposed here aims at working with an arbitrary noninteracting density of states (DOS) as input. Nevertheless, we intend to show that even for the solution of model Hamiltonians like, e.g., the Hubbard Hamiltonian, a DMFT scheme with a closed set of equations gained from a decoupling scheme is superior to the direct solution of that Hamiltonian with decoupling methods.

II. THEORY

The method of writing equations of motion (EOM) for the Anderson impurity model and decoupling them in order to close the system of equations has a long history.¹²⁻¹⁴ In the derivation of the integral equation for the solution of the infinite U Anderson impurity model we follow the approach and the decoupling scheme of Costi.¹⁵ The Hamiltonian for a mixed valent impurity is¹⁵

$$H = \sum_{kn} \varepsilon_k c_{kn}^+ c_{kn} + \sum_n E_{fn} X^{nn} + E_{f0} X^{00} + \sum_{kn} (V_{kn}^* c_{kn}^+ X^{0n} + V_{kn} X^{n0} c_{kn}), \quad (1)$$

where the Hubbard X operators $X^{pq} = |p\rangle\langle q|$ are projectors for impurity states $|p\rangle$ and $\langle q|$. They follow the (anti-) commutation rules $[X^{\alpha\beta}, X^{\gamma\delta}]_{\pm} = \delta_{\beta\gamma} X^{\alpha\delta} \pm \delta_{\delta\alpha} X^{\gamma\beta}$. We determine the equation of motion for the m -channel f -electron Green's function (GF) $F_m(\omega) = \langle\langle X^{0m}; X^{m0} \rangle\rangle$ by writing

$$\omega \langle \langle X^{0m}; X^{m0} \rangle \rangle = \langle [X^{0m}, X^{m0}]_+ \rangle + \langle \langle [X^{0m}, H]; X^{m0} \rangle \rangle \quad (2)$$

and evaluating the (anti-)commutators. [We follow the Zubarev notation $G_{A,B}(\omega) = \langle \langle A; B \rangle \rangle$. For the definition of the correlation $\langle \cdot \rangle$ see Eq. (16).] The result is

$$\begin{aligned} (\omega - \varepsilon_f) \langle \langle X^{0m}; X^{m0} \rangle \rangle &= \langle X^{00} + X^{mm} \rangle \\ &+ \sum_k V_k \langle \langle (X^{00} + X^{mm}) c_{km}; X^{m0} \rangle \rangle \\ &+ \sum_{\substack{k \\ n \neq m}} V_k \langle \langle X^{nm} c_{kn}; X^{m0} \rangle \rangle, \end{aligned} \quad (3)$$

assuming that the hybridization V_k does not depend on the z component m of the angular momentum J . The abbreviation $\varepsilon_f \equiv E_{f_m} - E_{f_0}$ was introduced. The averages over the X operators are $\langle X^{00} \rangle = 1 - n_f$ and $\langle X^{mm} \rangle = n_f/N$ where the total number of f electrons is calculated as

$$n_f = -\frac{N}{\pi} \int d\omega' f(\omega') F_m''(\omega'), \quad (4)$$

with the notation $F_m(\omega) = F_m'(\omega) + iF_m''(\omega)$. For the higher order Green's functions on the rhs of Eq. (3) we also write equations of motion:

$$\begin{aligned} (\omega - \varepsilon_k) \langle \langle (X^{00} + X^{mm}) c_{kn}; X^{m0} \rangle \rangle &= V_k \langle \langle X^{0m}; X^{m0} \rangle \rangle + \sum_{\substack{q \\ n \neq m}} V_q \langle \langle c_{qn}^+ X^{0n} c_{km}; X^{m0} \rangle \rangle \\ &+ \sum_{\substack{q \\ n \neq m}} V_q \langle \langle c_{qn} X^{n0} c_{km}; X^{m0} \rangle \rangle, \end{aligned} \quad (5)$$

$$\begin{aligned} (\omega - \varepsilon_k) \langle \langle X^{nm} c_{kn}; X^{m0} \rangle \rangle &= -\langle X^{n0} c_{kn} \rangle + \sum_q V_q \langle \langle X^{n0} c_{qm} c_{kn}; X^{m0} \rangle \rangle \\ &+ \sum_q V_q \langle \langle X^{0m} c_{qn}^+ c_{kn}; X^{m0} \rangle \rangle. \end{aligned} \quad (6)$$

We now employ the decoupling scheme already given in Ref. 15 that conserves the particle number and angular momentum ($n \neq m$ is assumed):

$$\langle \langle c_{qn}^+ X^{0n} c_{km}; X^{m0} \rangle \rangle \approx \langle c_{qn}^+ X^{0n} \rangle \langle \langle c_{km}; X^{m0} \rangle \rangle, \quad (7)$$

$$\langle \langle c_{qn} X^{n0} c_{km}; X^{m0} \rangle \rangle \approx \langle c_{qn} X^{n0} \rangle \langle \langle c_{km}; X^{m0} \rangle \rangle, \quad (8)$$

$$\langle \langle X^{n0} c_{qm} c_{kn}; X^{m0} \rangle \rangle \approx \langle c_{kn} X^{n0} \rangle \langle \langle c_{qm}; X^{m0} \rangle \rangle, \quad (9)$$

$$\langle \langle X^{0m} c_{qn}^+ c_{kn}; X^{m0} \rangle \rangle \approx \langle c_{qn}^+ c_{kn} \rangle \langle \langle X^{0m}; X^{m0} \rangle \rangle. \quad (10)$$

Note a sign difference in Eq. (9) with respect to Ref. 15. The Green's function $\langle \langle c_{qm}; X^{m0} \rangle \rangle$ appearing here can again be determined from its equation of motion,

$$\langle \langle c_{qm}; X^{m0} \rangle \rangle = \frac{V_q}{\omega - \varepsilon_q} \langle \langle X^{0m}; X^{m0} \rangle \rangle. \quad (11)$$

This leads to the equation from which the f electron Green's function can be determined:

$$F_m(\omega) = \frac{1 - n_f + \frac{n_f}{N} + I_1(\omega)}{\omega - \varepsilon_f - \Delta(\omega) + I_2(\omega) - \Delta(\omega) I_1(\omega)}, \quad (12)$$

with the sums over correlation functions,

$$I_1(\omega) = - \sum_{\substack{k \\ n \neq m}} \frac{V_k}{\omega - \varepsilon_k} \langle X^{n0} c_{kn} \rangle, \quad (13)$$

$$I_2(\omega) = - \sum_{\substack{kq \\ n \neq m}} \frac{V_k V_q}{\omega - \varepsilon_k} \langle c_{qn}^+ c_{kn} \rangle, \quad (14)$$

and the hybridization function

$$\Delta(\omega) = \sum_k \frac{V_k^2}{\omega - \varepsilon_k}. \quad (15)$$

In the degenerate models we study in this paper, the sums over n with $n \neq m$ simply lead to factors of $N-1$. The sums over k and q can be simplified further.

To that end, we replace the correlation functions by integrals over the imaginary part of the corresponding Green's function,

$$\langle c_{kn}^+ c_{qn} \rangle = -\frac{1}{\pi} \int d\omega' f(\omega') \text{Im} \langle \langle c_{qn}; c_{kn}^+ \rangle \rangle. \quad (16)$$

The conduction electron Green's function $\langle \langle c_{qn}; c_{kn}^+ \rangle \rangle$ is determined from its equation of motion,

$$\langle \langle c_{qn}; c_{kn}^+ \rangle \rangle = \frac{\delta_{kq}}{\omega - \varepsilon_q} + \frac{V_k V_q}{(\omega - \varepsilon_k)(\omega - \varepsilon_q)} \langle \langle X^{0n}; X^{n0} \rangle \rangle. \quad (17)$$

Now in order to simplify the sums in Eqs. (13) and (14), we employ the identity

$$\frac{1}{(\omega - \varepsilon)(\omega' - \varepsilon)} = \frac{1}{\omega' - \omega} \left[\frac{1}{\omega - \varepsilon} - \frac{1}{\omega' - \varepsilon} \right]. \quad (18)$$

This allows us to identify occurrences of the hybridization function (15), and we find

$$\begin{aligned} I_1(\omega) &= \frac{N-1}{\pi} \int d\omega' \frac{f(\omega')}{\omega' - \omega} [F_m''(\omega') \Delta(\omega) \\ &- \text{Im}\{F_m(\omega') \Delta(\omega')\}], \end{aligned} \quad (19)$$

$$\begin{aligned} I_2(\omega) &= \frac{N-1}{\pi} \int d\omega' \frac{f(\omega')}{\omega' - \omega} [-\Delta''(\omega') \\ &+ \Delta(\omega) \text{Im}\{F_m(\omega') \Delta(\omega')\} - \text{Im}\{F_m(\omega') \Delta(\omega')^2\}]. \end{aligned} \quad (20)$$

Equations (12) together with (19) and (20) and the definition of n_f (4) form an integral equation for $F_m(\omega)$ that can be solved iteratively. In order to compute the integrals of Eqs. (19) and (20) we introduce the following real functions:

$$A_m(\omega) = -f(\omega) \text{Im} F_m(\omega),$$

$$B(\omega) = f(\omega)\text{Im}\Delta(\omega),$$

$$C_m(\omega) = f(\omega)\text{Im}\{F_m(\omega)\Delta(\omega)\},$$

$$D_m(\omega) = f(\omega)\text{Im}\{F_m(\omega)\Delta(\omega)^2\}. \quad (21)$$

Now the integrals read as

$$I_1(\omega) = \frac{1}{\pi} \sum_{n \neq m} \left[\Delta(\omega) \int \frac{d\omega'}{\pi} \frac{A_m(\omega')}{\omega - \omega'} + \int \frac{d\omega'}{\pi} \frac{C_m(\omega')}{\omega - \omega'} \right],$$

$$I_2(\omega) = \frac{1}{\pi} \sum_{n \neq m} \left[\int \frac{d\omega'}{\pi} \frac{B(\omega')}{\omega - \omega'} - \Delta(\omega) \int \frac{d\omega'}{\pi} \frac{C_m(\omega')}{\omega - \omega'} + \int \frac{d\omega'}{\pi} \frac{D_m(\omega')}{\omega - \omega'} \right]. \quad (22)$$

Thus, the calculation of the integrals reduces to simple evaluation of Kramers-Kronig integrals. The imaginary part for example of the first such integral is $-i\pi A_m(\omega')$.

It turns out that this set of equations on the real frequency axis is solved easily for the Anderson impurity model, but as we add self-consistency conditions in order to solve more complicated models in the DMFT approximation, convergence depends strongly on a good initial guess of the solution. For this purpose, we write equations analogous to Eqs. (12), (19), (20), and (4) on the Matsubara axis. Matsubara Green's functions are much more smooth than their counterparts on the real frequency axis and thus converge more easily. Nevertheless, the calculation of the Green's function on the imaginary axis does not make the real axis calculation redundant: First, the analytic continuation to the real axis is only accurate for low frequencies due to a lack of high frequency information in the Matsubara Green's function. Second, the dependence of the imaginary frequency grid on temperature,

$$i\omega_n = (2n + 1)\pi T, \quad (23)$$

means that at high temperatures, the low frequency part of the Green's function is very badly resolved, while at very low temperatures, an inordinate number of imaginary frequencies is necessary to describe the Green's function for all frequencies for which it significantly differs from zero. This means that from a practical point of view, the Matsubara Green's function is best calculated at an intermediate temperature, providing via analytic continuation a sufficiently accurate initial guess for the iterative solution of Eq. (12) on the real axis. This problem of the Matsubara formulation is not related to the well known difficulty in performing analytic continuation to the real axis.

All equations of motion are almost unchanged when we go over to Matsubara frequency $i\omega_n$, e.g., Eq. (17) becomes

$$\langle\langle c_{kn}; c_{qn}^+ \rangle\rangle_{i\omega_n} = \frac{\delta_{kq}}{i\omega_n - \varepsilon_q} + \frac{V_k V_q}{(i\omega_n - \varepsilon_k)(i\omega_n - \varepsilon_q)} \langle\langle X^{0n}; X^{n0} \rangle\rangle_{i\omega_n}. \quad (24)$$

Correlations have to be calculated as

$$\langle c_{qn}^+ c_{kn} \rangle = T \sum_{i\omega_n} \langle\langle c_{kn}; c_{qn}^+ \rangle\rangle_{i\omega_n} e^{i\omega_n 0^+}, \quad (25)$$

which replaces Eq. (16) for that purpose. In order to simplify the equations, we employ the analog of Eq. (18), namely

$$\frac{1}{(i\omega_n - \varepsilon_k)(i\omega'_n - \varepsilon_k)} = \frac{1}{i\omega'_n - i\omega_n} \left\{ \frac{1}{i\omega_n - \varepsilon_k} - \frac{1}{i\omega'_n - \varepsilon_k} \right\}, \quad (26)$$

and we identify occurrences of the hybridization function,

$$\Delta(i\omega_n) = \sum_k \frac{V_k^2}{i\omega_n - \varepsilon_k}. \quad (27)$$

This leads to the system of equations

$$F_m(i\omega_n) = \frac{1 - n_f + \frac{n_f}{N} + S_1(i\omega_n)}{i\omega_n - \varepsilon_f - \Delta(i\omega_n)(1 + S_1(i\omega_n)) + S_2(i\omega_n)}, \quad (28)$$

with

$$S_1(i\omega_n) = T \sum_{\substack{l \neq m \\ i\omega'_n}} \frac{\Delta(i\omega'_n) - \Delta(i\omega_n)}{i\omega'_n - i\omega_n} F_l(i\omega'_n) e^{i\omega'_n 0^+}, \quad (29)$$

$$S_2(i\omega_n) = T \sum_{\substack{l \neq m \\ i\omega'_n}} \frac{\Delta(i\omega'_n) - \Delta(i\omega_n)}{i\omega'_n - i\omega_n} \{1 + \Delta(i\omega'_n) F_l(i\omega'_n)\} e^{i\omega'_n 0^+}, \quad (30)$$

$$n_f = NT \sum_{i\omega'_n} F_m(i\omega'_n) e^{i\omega'_n 0^+}. \quad (31)$$

With the replacement

$$T \sum_{i\omega'_n} K(i\omega'_n) e^{i\omega'_n 0^+} \rightarrow -\frac{1}{\pi} \int d\omega' f(\omega') \text{Im} K(\omega'), \quad (32)$$

we can easily recover Eqs. (19) and (20) from (29) and (30). It is important to note that good convergence of the self-consistent solution of the system of equations depends crucially on the proper treatment of the slowly decaying high frequency tails of the addends of Eqs. (29)–(31). A high frequency expansion of these addends was performed to determine the coefficients of the terms proportional to $1/i\omega_n$ and $1/(i\omega_n)^2$. These terms were subtracted from the sums, and their value was determined analytically.

The solution of the Anderson impurity model according to the closed system of Eqs. (12), (14), and (15) has been investigated in detail in Ref. 15 and in a slightly less general version in Ref. 13. It was found that the solution shows the emergence of a Kondo resonance at low temperature. The temperature scaling differs from the exact result of Haldane¹⁶ by a factor of 2 in the exponent and in the prefactor. It was shown by Luo *et al.*¹⁷ that by decoupling in a different way in the case of a degeneracy $N=2$ the temperature scaling can

even be improved. The intensity of the Kondo peak is below the value that would be required by the Friedel sum rule. This means that in contrast to methods like NCA that exceed the unitary limit for some parameter ranges, no unphysical self-energies are observed in the case of the decoupling approach.

A. Hubbard model

We now proceed to investigate the usefulness of the impurity solver detailed above in its application in the DMFT context. Our application of the method to three lattice models is an exploratory study concentrating on a small number of important properties only. It is not the intention of this article to go into detail for each of the three models. We first investigate the Hubbard model in order to study the quasi-particle scaling of the Hubbard band with degeneracy N .

We consider the Hubbard Hamiltonian,

$$H = - \sum_{ij\sigma} t_{ij} c_{i\sigma}^{\dagger} c_{j\sigma} - \mu \sum_{i\sigma} c_{i\sigma}^{\dagger} c_{i\sigma} + \frac{U}{2} \sum_{i\sigma\sigma'} c_{i\sigma}^{\dagger} c_{i\sigma} c_{i\sigma'}^{\dagger} c_{i\sigma'}, \quad (33)$$

where the spin and orbital index σ runs from 1 to N . For this model, we have to solve the AIM with the self-consistency condition

$$\Delta(i\omega_n) = t^2 G_{oo\sigma}(i\omega_n). \quad (34)$$

For the derivation of this equation, see Appendix A.

B. Anderson lattice

We study the application of the $U=\infty$ impurity solver to the Anderson lattice in order to learn how this new approach compares to the straightforward decoupling of the equations of motion for the periodic Anderson model.¹⁵ We consider the periodic Anderson Hamiltonian,

$$H_{\text{PAM}} = - \sum_{ij\sigma} t_{ij}^c c_{i\sigma}^{\dagger} c_{j\sigma} - \sum_{ij\sigma} t_{ij}^f f_{i\sigma}^{\dagger} f_{j\sigma} + \varepsilon_c \sum_{i\sigma} c_{i\sigma}^{\dagger} c_{i\sigma} + \varepsilon_f \sum_{i\sigma} f_{i\sigma}^{\dagger} f_{i\sigma} + \sum_{i\sigma} (V_{i\sigma} c_{i\sigma}^{\dagger} f_{i\sigma} + V_{i\sigma}^* f_{i\sigma}^{\dagger} c_{i\sigma}) + \frac{U}{2} \sum_{i\sigma\sigma'} f_{i\sigma}^{\dagger} f_{i\sigma} f_{i\sigma'}^{\dagger} f_{i\sigma'}. \quad (35)$$

In this case, the self-consistency condition for the f electron Green's function is

$$G_f^{\text{local}}(i\omega_n) = \int d\varepsilon \rho_p(\varepsilon) \left(i\omega_n + \mu - \varepsilon_f^0 - \Sigma_f(i\omega_n) - \frac{V(\varepsilon)^2}{i\omega_n + \mu - \varepsilon} \right)^{-1}. \quad (36)$$

Here, the self-energy is determined from the equation

$$\mathcal{G}_f^{-1}(i\omega_n) = G_f^{-1}(i\omega_n) + \Sigma(i\omega_n), \quad (37)$$

and the Weiss function $\mathcal{G}_0(i\omega_n)$ is related to the hybridization function $\Delta(i\omega_n)$ by

$$\mathcal{G}_0^{-1}(i\omega_n) = i\omega_n + \mu - \varepsilon_f^0 - \Delta(i\omega_n). \quad (38)$$

The derivation of these equations is contained in Appendix B.

C. pd model

In order to study the Mott transition with the $U=\infty$ impurity solver described above, we consider the Hamiltonian¹⁹

$$H = - \sum_{ij\sigma} V_{ij} [d_{i\sigma}^{\dagger} p_{j\sigma} + p_{j\sigma}^{\dagger} d_{i\sigma}] + \varepsilon_p \sum_{j\sigma} p_{j\sigma}^{\dagger} p_{j\sigma} + \varepsilon_d \sum_{i\sigma} d_{i\sigma}^{\dagger} d_{i\sigma} + U_d \sum_i d_{i\uparrow}^{\dagger} d_{i\uparrow} d_{i\downarrow}^{\dagger} d_{i\downarrow}. \quad (39)$$

This model, which we call a pd model here, has been proposed to study the physics of the Cu-O planes of the cuprates for which the interaction strength $U \approx 10$ eV on the Cu d orbitals is much higher than the charge transfer gap of $E_g \approx 2$ eV. In this situation the $U=\infty$ approximation is expected to be very good as the physics of the problem is weakly sensitive to the value of U ²⁰ provided that U is large enough. The Hamiltonian (39) is similar to the Anderson lattice Hamiltonian if the conduction electron dispersion is taken to be a constant $\varepsilon_k = \varepsilon_p$ and if the k dependence of the hybridization V_k is retained. This changes the local conduction electron Green's function:

$$G_d^{\text{local}}(i\omega_n) = \int d\varepsilon \rho_{pd}(\varepsilon) \left(i\omega_n + \mu - \varepsilon_d - \Sigma_d(i\omega_n) - \frac{\varepsilon^2}{i\omega_n + \mu - \varepsilon_p} \right)^{-1} = \zeta_p \int d\varepsilon \rho_{pd}(\varepsilon) (\zeta_p \zeta_d - \varepsilon^2)^{-1},$$

$$G_p^{\text{local}}(i\omega_n) = \int d\varepsilon \rho_{pd}(\varepsilon) \left(i\omega_n + \mu - \varepsilon_p - \frac{\varepsilon^2}{i\omega_n + \mu - \varepsilon_d - \Sigma_d(i\omega_n)} \right)^{-1} = \zeta_d \int d\varepsilon \rho_{pd}(\varepsilon) (\zeta_p \zeta_d - \varepsilon^2)^{-1}, \quad (40)$$

with the abbreviations $\zeta_p = i\omega_n + \mu - \varepsilon_p$ and $\zeta_d = i\omega_n + \mu - \varepsilon_d - \Sigma_d(i\omega_n)$. Here, $\rho_{pd}(\varepsilon)$ stands for the density of states associated with the hybridization V_k . Noting that

$$\int d\varepsilon \frac{\rho_{pd}(\varepsilon)}{x^2 - \varepsilon^2} = \frac{1}{2x} \left[\int d\varepsilon \frac{\rho_{pd}(\varepsilon)}{x - \varepsilon} + \int d\varepsilon \frac{\rho_{pd}(\varepsilon)}{x + \varepsilon} \right] = \frac{1}{2x} [\tilde{D}(x) - \tilde{D}(-x)] = \frac{\tilde{D}(x)}{x} \quad \text{for symmetric } \rho_{pd}(\varepsilon), \quad (41)$$

we can write $G_p^{\text{local}}(i\omega_n)$ and $G_d^{\text{local}}(i\omega_n)$ as Hilbert transforms:

$$G_p^{\text{local}}(i\omega_n) = \sqrt{\frac{\zeta_d}{\zeta_p}} \tilde{D}(\sqrt{\zeta_p \zeta_d}),$$

$$G_d^{\text{local}}(i\omega_n) = \sqrt{\frac{\zeta_p}{\zeta_d}} \tilde{D}(\sqrt{\zeta_p \zeta_d}). \quad (42)$$

We use a semicircular form for $\rho_{pd}(\varepsilon)$,

$$\rho_{pd}(\varepsilon) = \frac{1}{2\pi t_{pd}^2} \sqrt{4t_{pd}^2 - \varepsilon^2}, \quad (43)$$

where t_{pd} is the strength of the hybridization between p and d levels.

It is worth pointing out that this method reproduces an important aspect of the exact solution of the DMFT equations within the context of the pd model. Namely, it produces a first order phase transition between a metallic and an insulating phase, which is manifested by the existence of two DMFT solutions for the same range of parameters.

III. RESULTS

A. Hubbard model

First of all we test the performance of our impurity solver by comparing it with the results of exact diagonalization (ED). For this purpose, we employ the code published accompanying the review of the DMFT method in Ref. 1, modified to $U=\infty$. The Hubbard model is solved in the DMFT approximation. The self-consistency condition for the Hubbard model is realized by minimizing the function $f(\varepsilon_k, V_k) = \sum_n |t^2 G(i\omega_n) - \sum_k V_k^2 / (i\omega_n - \varepsilon_k)|$ with respect to the parameters ε_k and V_k . Here, the exact diagonalization has been performed with $N_s=6$ sites which are divided into one site for the impurity and five sites for the bath. Thus, the hybridization function $\Delta(i\omega_n)$ is represented with five poles. This leads to a finite number of poles instead of a smooth function in the spectral function as well. Figure 1 shows the comparison of the densities of f electrons as a function of the impurity position ε_f (which is related to the chemical potential by $\mu = -\varepsilon_f$). The comparison shows that at high temperature $T=0.5$, the results of exact diagonalization and EOM are virtually indistinguishable while for a lower temperature $T=0.03$, the densities differ slightly for impurity positions between -1 and 1 .

In Fig. 2, we compare the imaginary parts of the Green's function for a density of $n_f=0.84$. The slight differences in the n_f versus μ curves of Fig. 1 mean that this density is achieved for $\mu=0.6$ in the case of ED and for $\mu=0.53$ in the case of EOM. The imaginary parts of the Green's function on the Matsubara axis shown in the inset are very similar. Thus, the main figure shows the more demanding comparison of the densities of state. The continuous line represents the DOS from the EOM method gained by analytic continuation in the Padé approximation, while the long dashes stand for the EOM result on the real axis. The dashed curve with the five poles is the result of DMFT on the basis of exact diagonalization. The figure shows that the distribution of spectral weight between the Kondo peak around the Fermi level at

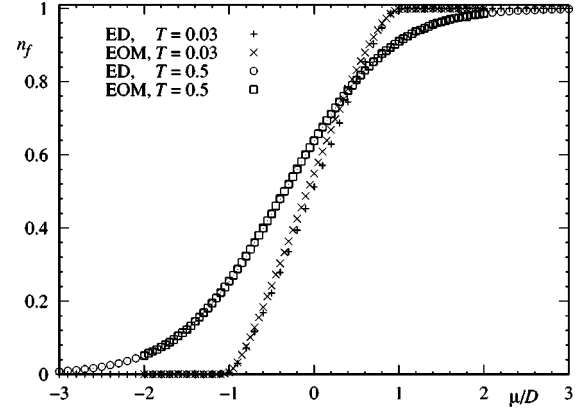


FIG. 1. Density of f electrons as a function of the chemical potential $\mu = -\varepsilon_f$ for exact diagonalization and the equation of motion method in comparison. The energy unit is the half bandwidth D . For the higher temperature $T=0.5$, the two methods agree extremely well, while for the lower temperature $T=0.03$, the exact diagonalization gives slightly lower densities at the same chemical potential $\mu = -\varepsilon_f$. Exact diagonalization was performed with 6 sites, and the Hubbard model was solved in the DMFT approximation.

$\omega=0$ and the Hubbard band is similar in both methods, but the EOM method leads to a better overall shape of the spectral function. We conclude that the EOM method results compare well with ED, giving us confidence that it is a useful approximation. Even for this low number of $N_s=6$ sites, the exact diagonalization requires an order of magnitude more CPU time than the EOM method.

Figure 3 shows the carrier density as a function of the impurity position ε_f . The impurity position corresponds to the chemical potential, only with opposite sign $\mu = -\varepsilon_f$. Due to the infinite interaction, the maximum filling is one electron per site. In other words, the upper Hubbard band that could hold a second electron at finite U has been pushed to infinite energy. While at low temperature $T=0.03$ the n_f versus μ curves at different degeneracies $N=2$ to $N=14$ nearly

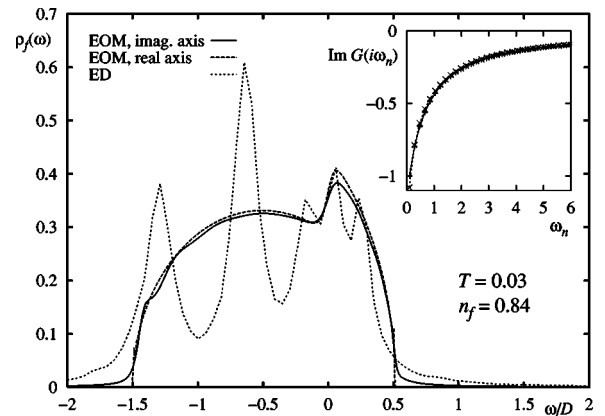


FIG. 2. Spectral functions (main figure) and an imaginary part of the Green's function (inset) from exact diagonalization and the equation of motion method in comparison. The temperature is $T=0.03$, the density of f electrons is $n_f=0.84$ for both methods. The two methods compare well, considering that the exact diagonalization with 5 bath sites has only limited resolution on the real axis.

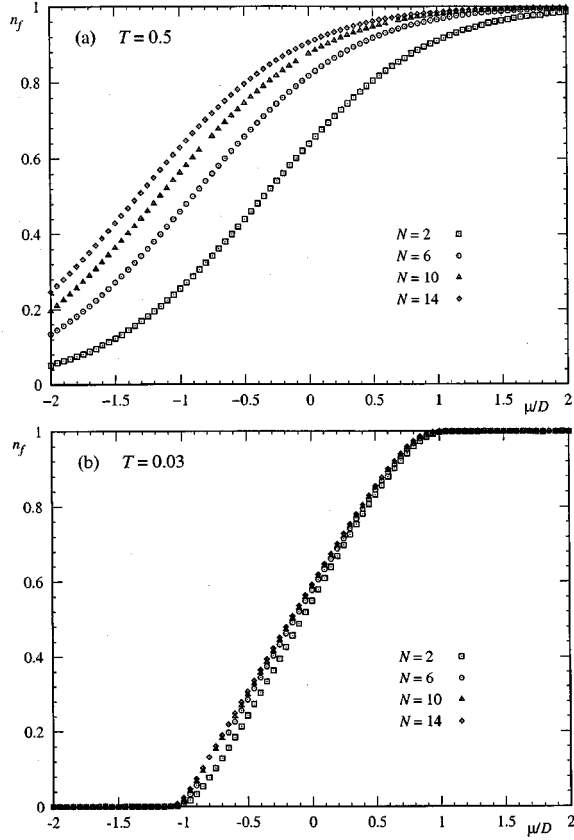


FIG. 3. Density n_f of f electrons as a function of the chemical potential μ for the infinite U Hubbard model. Energy is measured in units of a half bandwidth D . (a) At high temperature $T=0.5$, $n_f(\varepsilon_f)$ differs for different values of the degeneracy N . (b) At low temperature $T=0.03$, the $n_f(\varepsilon_f)$ for different N nearly coincide.

coincide [see Fig. 3(b)], they differ considerably at high temperature $T=0.5$ [see Fig. 3(a)].

In Fig. 4 we show examples of the spectral function for degeneracies between $N=2$ and $N=14$ for high and low temperature. While at $T=0.5$ the spectral function is nearly unstructured, at $T=0.003$ a broad Hubbard band and a quasiparticle resonance at zero frequency $\omega=0$ can be distinguished. The weight of the Hubbard band diminishes as $1/N$ as the degeneracy N increases while the intensity of the Kondo peaks remains nearly constant. Note that the spectral functions in Fig. 4 resulting from the DMFT self-consistency contain no spurious side bands as those calculated by directly decoupling the equations of motion produced by the Hubbard Hamiltonian.¹⁸ In our calculation, the imaginary part of the Green's function outside the Hubbard band and resonance is exactly zero.

B. Anderson lattice

Figure 5 shows examples for the conduction electron and the strongly correlated f electron spectral functions (dashed and full lines, respectively). In Fig. 5(a), the hybridization between the two bands is small ($V^2=0.01$) while in Fig. 5(b) it is rather large ($V^2=0.2$). Correspondingly, the conduction electron DOS shows only a small dip at the position of the

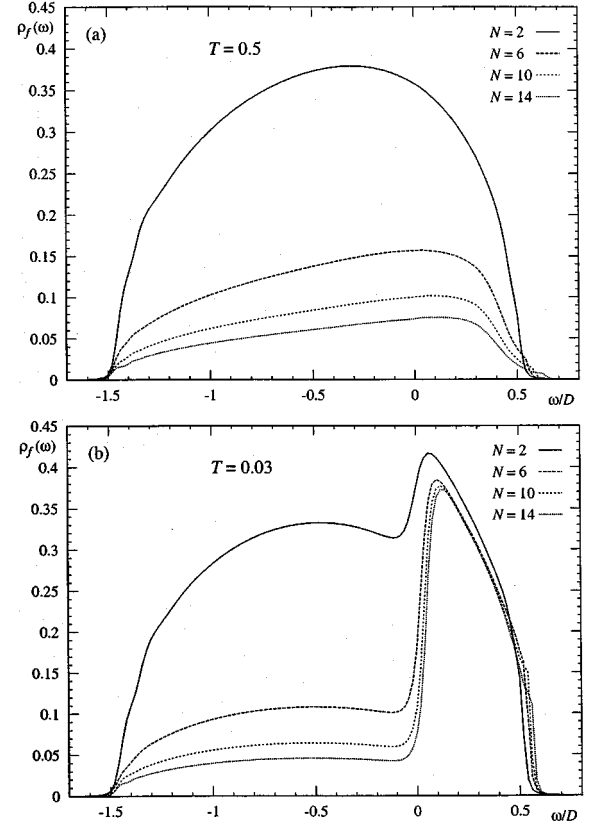


FIG. 4. Density of states $\rho_f(\omega)$ of f electrons for the infinite U Hubbard model. The energy unit is the half bandwidth D . (a) At high temperature $T=0.5$, there is no quasiparticle resonance at $\omega=0$. (b) At low temperature $T=0.03$, the quasiparticle resonance at $\omega=0$ is clearly developed. The weight of the Hubbard band is proportional to $1/N$.

band for a low value of the hybridization. Interestingly, we find a Kondo resonance at the Fermi level in the f electron DOS. This resonance was absent in the decoupling approach to the periodic Anderson model of Ref. 15.

C. pd model

We investigate the pd model Hamiltonian, Eq. (39), as a function of the separation $\Delta_0 = \varepsilon_p - \varepsilon_d$ and of the hybridization strength t_{pd} between the two bands. From the analysis in Ref. 19 of the finite U version of this model, we expect a metal insulator transition to occur at a fixed density $n_{tot}=1$ if we vary the level separation Δ_0 at a given t_{pd} . Figure 6(a) shows the result of this calculation at a fixed $t_{pd}=1$. The temperature was taken to be $T=0.01$. For level separations $\Delta_0=0$ and $\Delta_0=0.5$, the density n_{tot} around $n_{tot}=1$ changes smoothly as a function of chemical potential. But beginning with $\Delta_0=1.0$, a charge transfer gap $g_1 = \mu(n_{tot}=1^+) - \mu(n_{tot}=1^-)$ begins to open up. Thus, the physics discussed in Ref. 19 for finite values of U can be also found for $U=\infty$. The critical value at $t_{pd}=1$ is $\Delta_0=1$. Note that the $\Delta_0=4$, $U=8$ result in Fig. 1 of Ref. 19 compares well with the $\Delta_0=4$, $U=\infty$ curve of this work's Fig. 6(a). If we increase the hybridization strength to $t_{pd}=4$ [see Fig. 6(b)], we find that the

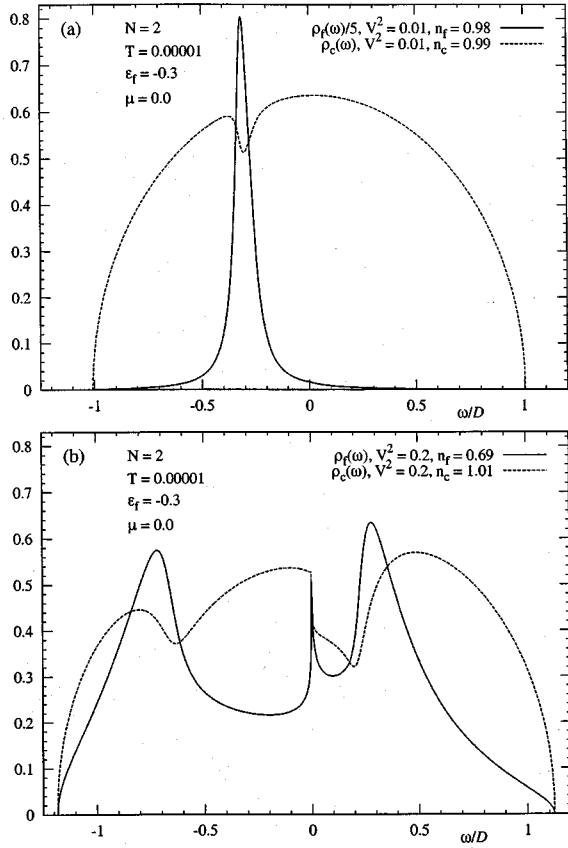


FIG. 5. Densities of states $\rho_f(\omega)$ and $\rho_c(\omega)$ of f and conduction electrons for the infinite U periodic Anderson model. (a) At a low hybridization $V^2=0.01$, the f electron Green's function is mainly a peak at the impurity position; there is no quasiparticle resonance at $\omega=0$. (b) At a high hybridization $V^2=0.2$, the Hubbard band of the f electron Green's function is split into two peaks, and the quasiparticle resonance at $\omega=0$ is clearly developed.

critical Δ_0 for the metal to charge transfer insulator increases to $\Delta_0 \approx 4$. In Fig. 6(a), we also note the transition at a total density $n_{tot}=2$ from a metal at higher level separation Δ_0 to a band insulator with a gap $g_2 = \mu(n_{tot}=2^+) - \mu(n_{tot}=2^-)$. For the higher value of the hybridization strength t_{pd} , the system is a band insulator at $n_{tot}=2$ for all studied level separations Δ_0 .

An important question in the metal to insulator transition of Fig. 6 concerns the existence of a coexistence region. We can show that such a coexistence is indeed found with our method. Figure 7 shows spectral functions for d and p electrons at a hybridization strength $t_{pd}=1$, a separation $\Delta_0 = \epsilon_p - \epsilon_d = 1$ and a chemical potential $\mu - \epsilon_d = 0.3$. The calculation was performed for a temperature of $T=10^{-5}$, and care was taken to resolve the sharp peak of the noninteracting Green's function $G_p(\omega)$ at $\epsilon_p=0.5$ with the help of a logarithmic grid. The full line shows the converged result of a direct calculation at $\mu - \epsilon_d = 0.3$. A quasiparticle peak at $\omega=0$ for both the correlated and the uncorrelated electrons makes this a metallic solution. The dashed line was obtained by starting the calculation in the insulating region at $\mu - \epsilon_d = 0.5$ and lowering the chemical potential in steps of 0.01. At $\mu - \epsilon_d = 0.3$, the solution is still insulating as no quasiparticle peak has formed.

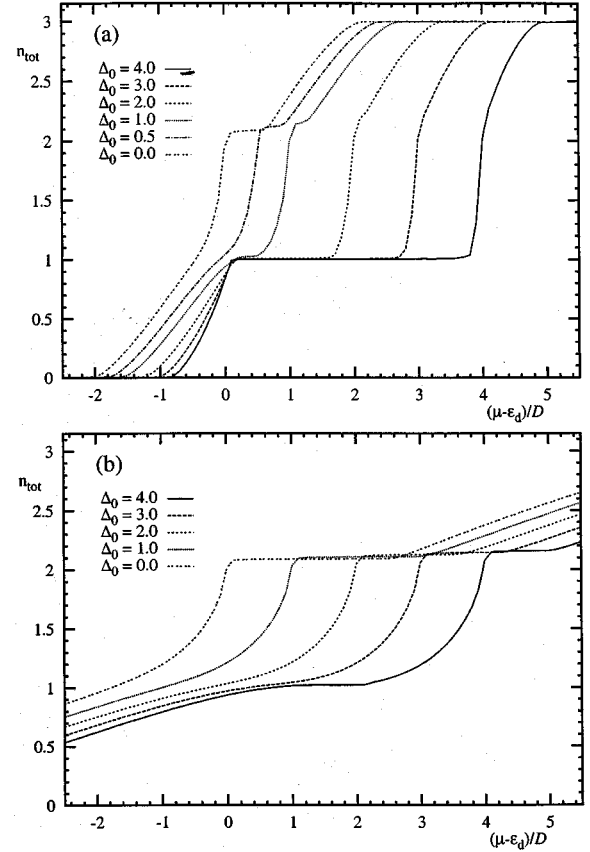


FIG. 6. The total density of electrons as a function of chemical potential for the pd model Hamiltonian (39). The hybridization strengths were (a) $t_{pd}=1$ and (b) $t_{pd}=4$. The plateaus at densities $n_{total}=1$ and $n_{total}=2$ correspond to the insulating phases.

IV. SUMMARY

A method to solve the Anderson impurity model with the help of equations of motion and decoupling has been tested for its suitability as an impurity solver in the framework of dynamical mean field theory. The application to three lattice models in infinite dimensions and for infinite interaction strength U shows very encouraging results. In the application to the Hubbard model, we see a correct quasiparticle scaling of the Hubbard band with respect to the degeneracy. In the periodic Anderson model, we find a Kondo resonance which is absent in a direct decoupling of the equations of motion. This underlines the usefulness of the approach chosen here: To use a decoupling scheme for the solution of the Anderson impurity model which is then employed to solve lattice models in the DMFT approximation. Interestingly, the application of our approach to the pd model yields a coexistence of the insulating and metallic phases. The extension of the $U = \infty$ approach discussed here to finite values of the interaction strength U is possible and in preparation. The numerical efficiency of the method makes an application in an LDA +DMFT context feasible.

ACKNOWLEDGMENTS

H.O.J. gratefully acknowledges support from the Deutsche Forschungsgemeinschaft (DFG) through the Emmy

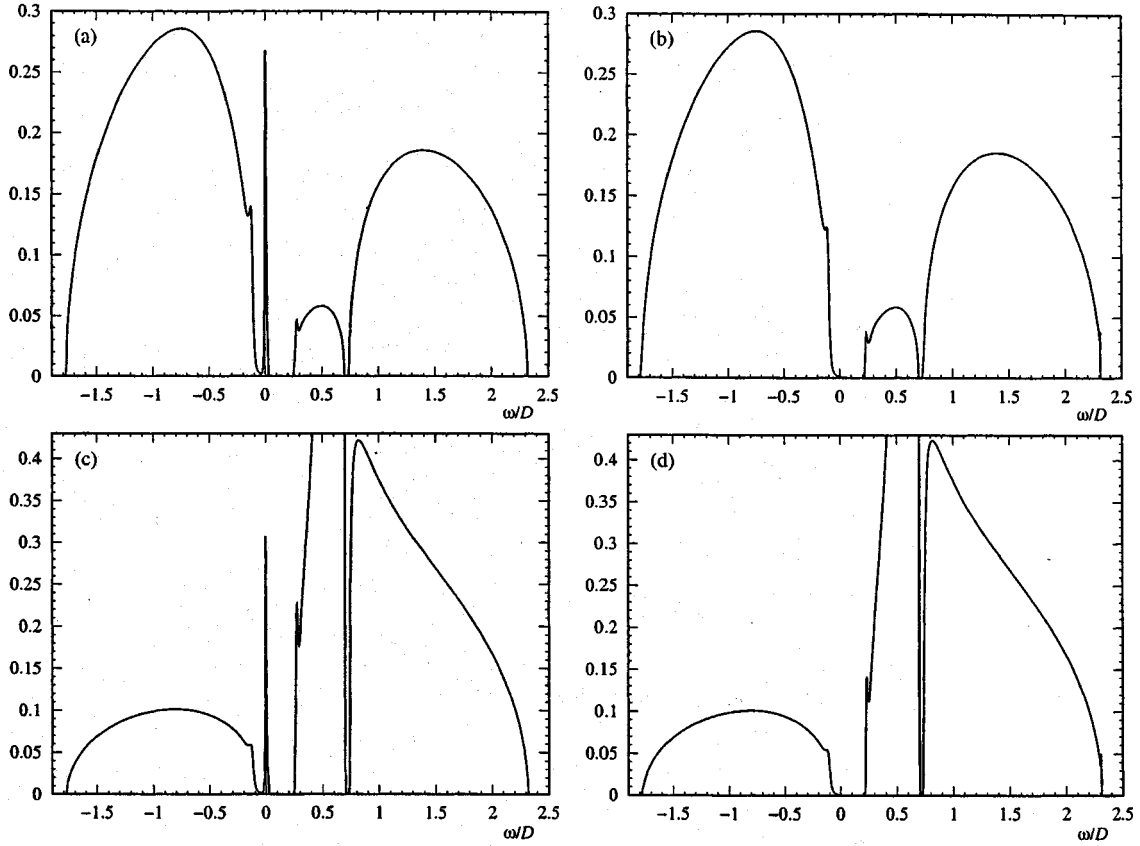


FIG. 7. The spectral function for the pd model Hamiltonian (39) showing the coexistence of a metallic and an insulating phase. The hybridization strength was $t_{pd}=1$, the pd separation $\Delta_0=1$. (a) and (b) show the correlated d spectral function, (c) and (d) the uncorrelated p spectral function. In the case of (a) and (c), the solution was calculated directly for a chemical potential $\mu-\varepsilon_d=0.3$ and the solution is metallic due to the sharp Kondo resonance at the Fermi level. In the case of (b) and (d), the chemical potential was changed to $\mu-\varepsilon_d=0.3$ in small steps, starting from an insulating solution. The resulting DOS is still insulating. Note that in (c) and (d) the sharp peak of the noninteracting DOS at $\varepsilon_p=0.5$ is not shown.

Noether Programme. He is also thankful for inspiring discussions with Kristjan Haule, Theo Costi and Sarma Kancharla. G.K. is supported by NSF DMR-0096462.

APPENDIX A: DMFT SELF-CONSISTENCY CONDITION FOR THE HUBBARD MODEL

The partition function corresponding to the Hamiltonian of Eq. (33) is

$$Z = \int \prod_i \mathcal{D}\bar{c}_{i\sigma} \mathcal{D}c_{i\sigma} e^{-S}, \quad (\text{A1})$$

with the action

$$S = \int_0^\beta d\tau \sum_{i\sigma} \bar{c}_{i\sigma}(\tau) \frac{\partial}{\partial \tau} c_{i\sigma}(\tau) + \int_0^\beta d\tau \left[- \sum_{ij\sigma} t_{ij} \bar{c}_{i\sigma}(\tau) c_{j\sigma}(\tau) - \mu \sum_{i\sigma} \bar{c}_{i\sigma}(\tau) c_{i\sigma}(\tau) + \frac{U}{2} \sum_{\substack{i\sigma\sigma' \\ \sigma \neq \sigma'}} \bar{c}_{i\sigma}(\tau) c_{i\sigma}(\tau) \bar{c}_{i\sigma'}(\tau) c_{i\sigma'}(\tau) \right], \quad (\text{A2})$$

where the Fermion operators $c_{i\sigma}^+$, $c_{i\sigma}$ of the Hamiltonian have

been replaced by Grassmann variables $\bar{c}_{i\sigma}(\tau)$, $c_{i\sigma}(\tau)$.

The cavity method now requires that we focus on one site $i=o$ and separate the Hamiltonian (33) into three parts, one relating to site o only, one connecting this site to the lattice, and one for the lattice with site o removed,

$$H = H_o + H_c + H^{(o)}, \quad (\text{A3})$$

$$H_o = -\mu \sum_{\sigma} c_{o\sigma}^+ c_{o\sigma} + \frac{U}{2} \sum_{\substack{\sigma\sigma' \\ \sigma \neq \sigma'}} c_{o\sigma}^+ c_{o\sigma} c_{o\sigma'}^+ c_{o\sigma'}, \quad (\text{A4})$$

$$H_c = - \sum_{i\sigma} [t_{io} c_{i\sigma}^+ c_{o\sigma} + t_{oi} c_{o\sigma}^+ c_{i\sigma}], \quad (\text{A5})$$

$$H^{(o)} = - \sum_{\substack{ij\sigma \\ i \neq o, j \neq o}} t_{ij} c_{i\sigma}^+ c_{j\sigma} - \mu \sum_{i \neq o\sigma} c_{i\sigma}^+ c_{i\sigma} + \frac{U}{2} \sum_{\substack{i \neq o\sigma\sigma' \\ \sigma \neq \sigma'}} c_{i\sigma}^+ c_{i\sigma} c_{i\sigma'}^+ c_{i\sigma'}. \quad (\text{A6})$$

The three parts of the Hamiltonian correspond to the action S_o of site o , the action ΔS for the interaction between site o

and the lattice and the action $S^{(o)}$ of the lattice without site o :

$$S_o = \int_0^\beta d\tau \left[\sum_{\sigma} \bar{c}_{o\sigma}(\tau) \left(\frac{\partial}{\partial \tau} - \mu \right) c_{o\sigma}(\tau) + \frac{U}{2} \sum_{\substack{\sigma\sigma' \\ \sigma \neq \sigma'}} \bar{c}_{o\sigma}(\tau) c_{o\sigma}(\tau) \bar{c}_{o\sigma'}(\tau) c_{o\sigma'}(\tau) \right], \quad (\text{A7})$$

$$\Delta S = - \int_0^\beta d\tau \left[\sum_{i\sigma} t_{io} \bar{c}_{i\sigma}(\tau) c_{o\sigma}(\tau) + t_{oi} \bar{c}_{o\sigma}(\tau) c_{i\sigma}(\tau) \right], \quad (\text{A8})$$

$$S^{(o)} = \int_0^\beta d\tau \left[\sum_{i \neq o\sigma} \bar{c}_{i\sigma}(\tau) \left(\frac{\partial}{\partial \tau} - \mu \right) c_{i\sigma}(\tau) - \sum_{i \neq o, j \neq o\sigma} t_{ij} \bar{c}_{i\sigma}(\tau) c_{j\sigma}(\tau) + \frac{U}{2} \sum_{\substack{i \neq o\sigma\sigma' \\ \sigma \neq \sigma'}} \bar{c}_{i\sigma}(\tau) c_{i\sigma}(\tau) \bar{c}_{i\sigma'}(\tau) c_{i\sigma'}(\tau) \right]. \quad (\text{A9})$$

The aim is now to integrate out all lattice degrees of freedom except those of site o in order to find the effective dynamics at site o . In that process, the action S_o remains unchanged, the terms of ΔS are expanded in terms of the hopping t which becomes small with increasing dimension and averaged with respect to the action $S^{(o)}$. Defining $\Delta S(\tau)$ via $\Delta S = \int_0^\beta d\tau \Delta S(\tau)$ the partition function is

$$Z = \int \mathcal{D}\bar{c}_{o\sigma} \mathcal{D}c_{o\sigma} e^{-S_o} \int \prod_{i \neq o} \mathcal{D}\bar{c}_{i\sigma} \mathcal{D}c_{i\sigma} e^{-S^{(o)}} e^{-\int_0^\beta d\tau \Delta S(\tau)}. \quad (\text{A10})$$

Now we can expand the last exponential function as

$$e^{-\int_0^\beta d\tau \Delta S(\tau)} = 1 - \int_0^\beta d\tau \Delta S(\tau) + \frac{1}{2!} \int_0^\beta d\tau_1 \int_0^\beta d\tau_2 \Delta S(\tau_1) \Delta S(\tau_2) - \dots. \quad (\text{A11})$$

Taking into account that in general an operator average with respect to an action S can be expressed as

$$\langle A \rangle_S = \frac{\int \prod_i \mathcal{D}\bar{c}_\alpha \mathcal{D}c_\alpha e^{-S} A[\bar{c}_\alpha, c_\alpha]}{\int \prod_i \mathcal{D}\bar{c}_\alpha \mathcal{D}c_\alpha e^{-S}} = Z_S^{-1} \int \prod_i \mathcal{D}\bar{c}_\alpha \mathcal{D}c_\alpha e^{-S} A[\bar{c}_\alpha, c_\alpha], \quad (\text{A12})$$

we can consider the second functional integral in (A10) to average the terms of the expansion (A11) with respect to the lattice action $S^{(o)}$:

$$Z = \int \prod_i \mathcal{D}\bar{c}_{o\sigma} \mathcal{D}c_{o\sigma} e^{-S_o} Z_{S^{(o)}} \left\{ 1 - \int_0^\beta d\tau \langle \Delta S(\tau) \rangle_{S^{(o)}} + \frac{1}{2!} \int_0^\beta d\tau_1 \int_0^\beta d\tau_2 \langle \Delta S(\tau_1) \Delta S(\tau_2) \rangle_{S^{(o)}} - \dots \right\}. \quad (\text{A13})$$

Here, the partition function of the lattice without site o is abbreviated as

$$Z_{S^{(o)}} = \int \prod_i \mathcal{D}\bar{c}_\alpha \mathcal{D}c_\alpha e^{-S^{(o)}}. \quad (\text{A14})$$

Now the terms in (A13) with odd powers of ΔS will average to zero. For example,

$$\langle \Delta S(\tau) \rangle_{S^{(o)}} = \sum_{i\sigma} t_{io} \langle \bar{c}_{i\sigma}(\tau) \rangle_{S^{(o)}} c_{o\sigma}(\tau) + t_{oi} \bar{c}_{o\sigma}(\tau) \langle c_{i\sigma}(\tau) \rangle_{S^{(o)}} = 0, \quad (\text{A15})$$

because the average $\langle \rangle_{S^{(o)}}$ acts on all sites except o . The next average in (A13) yields

$$\begin{aligned} \langle \Delta S(\tau_1) \Delta S(\tau_2) \rangle_{S^{(o)}} &= \left\langle T_\tau \left[\sum_{i\sigma} t_{io} \bar{c}_{i\sigma}(\tau_1) c_{o\sigma}(\tau_1) + t_{oi} \bar{c}_{o\sigma}(\tau_1) c_{i\sigma}(\tau_1) \right] \times \left[\sum_{j\sigma'} t_{jo} \bar{c}_{j\sigma'}(\tau_2) c_{o\sigma'}(\tau_2) + t_{oj} \bar{c}_{o\sigma'}(\tau_2) c_{j\sigma'}(\tau_2) \right] \right\rangle_{S^{(o)}} \\ &= \sum_{ij\sigma\sigma'} t_{io} t_{oj} c_{o\sigma}(\tau_1) \langle T_\tau \bar{c}_{i\sigma}(\tau_1) c_{j\sigma'}(\tau_2) \rangle_{S^{(o)}} \bar{c}_{o\sigma'}(\tau_2) + \sum_{ij\sigma\sigma'} t_{oi} t_{jo} \bar{c}_{o\sigma}(\tau_1) \langle T_\tau c_{i\sigma}(\tau_1) \bar{c}_{j\sigma'}(\tau_2) \rangle_{S^{(o)}} c_{o\sigma'}(\tau_2) \\ &= 2 \sum_{ij\sigma\sigma'} t_{io} t_{oj} \bar{c}_{o\sigma}(\tau_1) \langle T_\tau c_{i\sigma}(\tau_1) \bar{c}_{j\sigma'}(\tau_2) \rangle_{S^{(o)}} c_{o\sigma'}(\tau_2) \\ &= 2 \sum_{ij\sigma} t_{io} t_{oj} \bar{c}_{o\sigma}(\tau_1) \langle T_\tau c_{i\sigma}(\tau_1) \bar{c}_{j\sigma}(\tau_2) \rangle_{S^{(o)}} c_{o\sigma}(\tau_2) \\ &= -2 \sum_{ij\sigma} t_{io} t_{oj} \bar{c}_{o\sigma}(\tau_1) G_{ij\sigma}^{(o)}(\tau_1 - \tau_2) c_{o\sigma}(\tau_2). \end{aligned} \quad (\text{A16})$$

The imaginary time ordering operator T_τ enters because the path integral leads to imaginary time ordering. Only terms with $\sigma=\sigma'$ contribute as we are considering a paramagnetic state and thus $\langle T_\tau c_{i\sigma}(\tau_1)\bar{c}_{j\sigma'}(\tau_2)\rangle_{S^{(o)}} = \delta_{\sigma\sigma'}\langle T_\tau c_{i\sigma}(\tau_1)\bar{c}_{j\sigma}(\tau_2)\rangle_{S^{(o)}}$. We have identified the average with the cavity Green's function $G_{ij\sigma}^{(o)}(\tau_1-\tau_2) = -\langle T_\tau c_{i\sigma}(\tau_1)c_{j\sigma}^+(\tau_2)\rangle_{S^{(o)}}$, i.e., the Green's function of the Hubbard model without the site o . Now we have for the partition function,

$$Z = \int \prod_\sigma \mathcal{D}\bar{c}_{o\sigma} \mathcal{D}c_{o\sigma} e^{-S_o Z_{S^{(o)}}} \left\{ 1 - \int_0^\beta d\tau_1 \int_0^\beta d\tau_2 \times \sum_{ij\sigma} t_{io} t_{oj} \bar{c}_{o\sigma}(\tau_1) c_{o\sigma}(\tau_2) G_{ij\sigma}^{(o)}(\tau_1 - \tau_2) + \dots \right\}. \quad (\text{A17})$$

We would like to write the bracket $\{ \}$ in (A17) again as an exponential function in order to identify an effective action S_{eff} :

$$Z = \int \prod_i \mathcal{D}\bar{c}_{o\sigma} \mathcal{D}c_{o\sigma} e^{-S_o Z_{S^{(o)}}} \exp \left\{ - \sum_{n=1}^{\infty} \sum_\sigma \int_0^\beta d\tau_1 \cdots \int_0^\beta d\tau_{2n} \bar{c}_{o\sigma}(\tau_1) \cdots \bar{c}_{o\sigma}(\tau_{2n-1}) c_{o\sigma}(\tau_2) \cdots c_{o\sigma}(\tau_{2n}) \times \sum_{\substack{i_1, \dots, i_n \\ j_1, \dots, j_n}} t_{i_1 o} \cdots t_{i_n o} t_{o j_1} \cdots t_{o j_n} G_{i_1 \dots i_n j_1 \dots j_n}^{(o)}(\tau_1 \cdots \tau_{2n-1}, \tau_2 \cdots \tau_{2n}) \right\}. \quad (\text{A20})$$

All terms but the first in this sum over n turn out to be at least of order $1/d$ so that they vanish in the limit of infinite dimension $d=\infty$. Thus, in this limit we find for the effective action,

$$S_{\text{eff}} = S_o + \sum_\sigma \int_0^\beta d\tau_1 \int_0^\beta d\tau_2 \bar{c}_{o\sigma}(\tau_1) c_{o\sigma}(\tau_2) \times \sum_{ij} t_{io} t_{oj} G_{ij\sigma}^{(o)}(\tau_1 - \tau_2) = \int_0^\beta d\tau \left[\sum_\sigma \bar{c}_{o\sigma}(\tau) \left(\frac{\partial}{\partial \tau} - \mu \right) c_{o\sigma}(\tau) + \frac{U}{2} \sum_{\substack{\sigma\sigma' \\ \sigma \neq \sigma'}} \bar{c}_{o\sigma}(\tau) c_{o\sigma}(\tau) \bar{c}_{o\sigma'}(\tau) c_{o\sigma'}(\tau) \right] + \sum_\sigma \int_0^\beta d\tau_1 \int_0^\beta d\tau_2 \bar{c}_{o\sigma}(\tau_1) c_{o\sigma}(\tau_2) \sum_{ij} t_{io} t_{oj} G_{ij\sigma}^{(o)}(\tau_1 - \tau_2), \quad (\text{A21})$$

and introducing the Weiss field,

$$Z = \int \prod_i \mathcal{D}\bar{c}_{o\sigma} \mathcal{D}c_{o\sigma} e^{-S_{\text{eff}}}. \quad (\text{A18})$$

Noting that the next term in the expansion of (A17) would read as

$$\int_0^\beta d\tau_1 \int_0^\beta d\tau_2 \int_0^\beta d\tau_3 \int_0^\beta d\tau_4 \times \sum_{i_1 i_2 j_1 j_2 \sigma} \bar{c}_{o\sigma}(\tau_1) \bar{c}_{o\sigma}(\tau_3) c_{o\sigma}(\tau_2) c_{o\sigma}(\tau_4) \times t_{i_1 o} t_{i_2 o} t_{o j_1} t_{o j_2} G_{i_1 i_2 j_1 j_2}^{(o)}(\tau_1 \tau_3, \tau_2 \tau_4), \quad (\text{A19})$$

we can write for the partition function (A17)

$$\mathcal{G}_\sigma^{-1}(\tau_1 - \tau_2) = - \left(\frac{\partial}{\partial \tau_1} - \mu \right) \delta_{\tau_1 \tau_2} - \sum_{ij} t_{io} t_{oj} G_{ij\sigma}^{(o)}(\tau_1 - \tau_2), \quad (\text{A22})$$

we finally get

$$S_{\text{eff}} = - \sum_\sigma \int_0^\beta d\tau_1 \int_0^\beta d\tau_2 \bar{c}_{o\sigma}(\tau_1) \mathcal{G}_\sigma^{-1}(\tau_1 - \tau_2) c_{o\sigma}(\tau_2) + \int_0^\beta d\tau \frac{U}{2} \sum_{\substack{\sigma\sigma' \\ \sigma \neq \sigma'}} \bar{c}_{o\sigma}(\tau) c_{o\sigma}(\tau) \bar{c}_{o\sigma'}(\tau) c_{o\sigma'}(\tau). \quad (\text{A23})$$

The equation

$$G_{ij\sigma}^{(o)} = G_{ij\sigma} - G_{io\sigma} G_{oo\sigma}^{-1} G_{oj\sigma} \quad (\text{A24})$$

is needed to relate the cavity Green's function to the Green's function of the lattice $G_{ij\sigma}$. Going from imaginary time to imaginary frequency and combining with (A24), the Weiss function (A22) reads as

$$\begin{aligned}
 \mathcal{G}_\sigma^{-1}(i\omega_n) &= i\omega_n + \mu - \sum_{ij} t_{io}t_{oj}G_{ij\sigma}^{(o)}(i\omega_n) \\
 &= i\omega_n + \mu - \sum_{ij} t_{io}t_{oj} \left[G_{ij\sigma}(i\omega_n) \right. \\
 &\quad \left. - G_{io\sigma}(i\omega_n)G_{oo\sigma}^{-1}(i\omega_n)G_{oj\sigma}(i\omega_n) \right]. \quad (\text{A25})
 \end{aligned}$$

If we now go from real space to k space we can simplify this equation. Introducing the Fourier transform $G_{k\sigma}$ via

$$G_{ij\sigma}(i\omega_n) = \sum_k e^{ikR_{ij}} G_{k\sigma}(i\omega_n), \quad (\text{A26})$$

we find

$$\begin{aligned}
 \sum_i t_{io}G_{io\sigma}(i\omega_n) &= \sum_i t_{io} \sum_k e^{ikR_{io}} G_{k\sigma}(i\omega_n) = \sum_k \varepsilon_k G_{k\sigma}(i\omega_n), \\
 \sum_{ij} t_{io}t_{oj}G_{ij\sigma}(i\omega_n) &= \sum_{ij} t_{io}t_{oj} \sum_k e^{ikR_{ij}} G_{k\sigma}(i\omega_n) \\
 &= \sum_k \sum_i t_{io} e^{ikR_{io}} \sum_j t_{oj} e^{ikR_{oj}} G_{k\sigma}(i\omega_n) \\
 &= \sum_k \varepsilon_k^2 G_{k\sigma}(i\omega_n). \quad (\text{A27})
 \end{aligned}$$

In the general form of the Green's function $G_{k\sigma}^{-1}(i\omega_n) = i\omega_n + \mu - \varepsilon_k - \sum_\sigma(i\omega_n)$ we introduce the abbreviation $\xi = i\omega_n + \mu - \sum_\sigma(i\omega_n)$ to get $G_{k\sigma}^{-1}(i\omega_n) = \xi - \varepsilon_k$ and determine the sums

$$\begin{aligned}
 \sum_k \varepsilon_k G_{k\sigma}(i\omega_n) &= \sum_k \frac{\varepsilon_k}{\xi - \varepsilon_k} \\
 &= \sum_k \frac{\varepsilon_k - \xi + \xi}{\xi - \varepsilon_k} = -1 + \sum_k \frac{\xi}{\xi - \varepsilon_k} \\
 &= -1 + \xi \sum_k G_{k\sigma}(i\omega_n) = -1 + \xi G_{oo\sigma}(i\omega_n), \\
 \sum_k \varepsilon_k^2 G_{k\sigma}(i\omega_n) &= \sum_k \frac{\varepsilon_k^2}{\xi - \varepsilon_k} = \sum_k \frac{\varepsilon_k(\varepsilon_k - \xi) + \varepsilon_k \xi}{\xi - \varepsilon_k} \\
 &= \sum_k \varepsilon_k + \xi \sum_k \frac{\varepsilon_k}{\xi - \varepsilon_k} \\
 &= \xi[-1 + \xi G_{oo\sigma}(i\omega_n)] = -\xi + \xi^2 G_{oo\sigma}(i\omega_n). \quad (\text{A28})
 \end{aligned}$$

With this, the Weiss function (A25) becomes

$$\begin{aligned}
 \mathcal{G}_\sigma^{-1}(i\omega_n) &= i\omega_n + \mu - \sum_k \varepsilon_k^2 G_{k\sigma}(i\omega_n) \\
 &\quad + \left(\sum_k \varepsilon_k G_{k\sigma}(i\omega_n) \right)^2 G_{oo\sigma}^{-1}(i\omega_n) \\
 &= i\omega_n + \mu + \xi - \xi^2 G_{oo\sigma}(i\omega_n) + [-1 + \xi G_{oo\sigma}(i\omega_n)] \\
 &\quad \times [-G_{oo\sigma}^{-1}(i\omega_n) + \xi] = i\omega_n + \mu - \xi + G_{oo\sigma}^{-1}(i\omega_n) \\
 &= \sum_\sigma(i\omega_n) + G_{oo\sigma}^{-1}(i\omega_n). \quad (\text{A29})
 \end{aligned}$$

This equation $G_{oo\sigma}^{-1}(i\omega_n) = \mathcal{G}_\sigma^{-1}(i\omega_n) - \sum_\sigma(i\omega_n)$ is the Dyson equation for the local Green's function.

The effective action (A23) can now be interpreted in terms of the Anderson impurity model, i.e., the Anderson impurity model gives rise to an action which becomes identical to (A23) if an additional self-consistency condition is fulfilled. The Hamiltonian for the Anderson impurity model is

$$\begin{aligned}
 H &= \sum_{k\sigma} \varepsilon_k c_{k\sigma}^\dagger c_{k\sigma} + \sum_{k\sigma} (V_k c_{k\sigma}^\dagger f_\sigma + V_k^* f_\sigma^\dagger c_{k\sigma}) - \sum_\sigma \mu f_\sigma^\dagger f_\sigma \\
 &\quad + \frac{U}{2} \sum_{\substack{\sigma\sigma' \\ \sigma \neq \sigma'}} f_\sigma^\dagger f_\sigma^\dagger f_{\sigma'} f_{\sigma'}, \quad (\text{A30})
 \end{aligned}$$

where σ runs from 1 to the degeneracy N . The action corresponding to this Hamiltonian will consist of a purely local part S_o concerning only the f electrons,

$$\begin{aligned}
 S_o &= \int_0^\beta d\tau \left[\sum_\sigma \bar{f}_\sigma(\tau) \left(\frac{\partial}{\partial \tau} - \mu \right) f_\sigma(\tau) \right. \\
 &\quad \left. + \frac{U}{2} \sum_{\substack{\sigma\sigma' \\ \sigma \neq \sigma'}} \bar{f}_\sigma(\tau) f_\sigma(\tau) \bar{f}_{\sigma'}(\tau) f_{\sigma'}(\tau) \right], \quad (\text{A31})
 \end{aligned}$$

and a part involving conduction band electrons that can be integrated out

$$\begin{aligned}
 S &= S_o + \int_0^\beta d\tau \sum_{k\sigma} \left[\bar{c}_{k\sigma}(\tau) \left(\frac{\partial}{\partial \tau} + \varepsilon_k \right) c_{k\sigma}(\tau) + V_k \bar{c}_{k\sigma}(\tau) f_\sigma(\tau) \right. \\
 &\quad \left. + V_k^* \bar{f}_\sigma(\tau) c_{k\sigma}(\tau) \right]. \quad (\text{A32})
 \end{aligned}$$

Now the partition function for the Hamiltonian (A30) is

$$\begin{aligned}
 Z &= \int \mathcal{D}\bar{f}_\sigma \mathcal{D}f_\sigma \int \prod_i \mathcal{D}\bar{c}_{i\sigma} \mathcal{D}c_{i\sigma} e^{-S} \\
 &= \int \mathcal{D}\bar{f}_\sigma \mathcal{D}f_\sigma e^{-S_o} \int \prod_i \mathcal{D}\bar{c}_{i\sigma} \mathcal{D}c_{i\sigma} \exp \left\{ \int_0^\beta d\tau \sum_{k\sigma} \left[\bar{c}_{k\sigma}(\tau) \right. \right. \\
 &\quad \left. \left. \times \left(\frac{\partial}{\partial \tau} + \varepsilon_k \right) c_{k\sigma}(\tau) + V_k \bar{c}_{k\sigma}(\tau) f_\sigma(\tau) + V_k^* \bar{f}_\sigma(\tau) c_{k\sigma}(\tau) \right] \right\} \\
 &= \int \mathcal{D}\bar{f}_\sigma \mathcal{D}f_\sigma e^{-S_o} \prod_k \det \left(\frac{\partial}{\partial \tau} + \varepsilon_k \right) \\
 &\quad \times \exp \left\{ \sum_{k\sigma} \int_0^\beta d\tau_1 \int_0^\beta d\tau_2 \bar{f}_\sigma(\tau_1) V_k^* V_k \right. \\
 &\quad \left. \times \left(\frac{\partial}{\partial \tau_1} + \varepsilon_k \right)^{-1} \delta_{\tau_1 \tau_2} f_\sigma(\tau_2) \right\}. \quad (\text{A33})
 \end{aligned}$$

In the last step, the terms involving f electrons $V_k^* \bar{f}_\sigma(\tau)$ and $V_k f_\sigma(\tau)$ were taken as source terms, which makes the term in the exponent a Gaussian integral that can be evaluated directly. The determinant constitutes a constant factor in the partition function that does not concern us here. We are left with an action for the f electrons that reads as

$$\begin{aligned}
S_f = & \int_0^\beta d\tau_1 \int_0^\beta d\tau_2 \sum_\sigma \bar{f}_\sigma(\tau_1) \left[\left(\frac{\partial}{\partial \tau_1} - \mu \right) \delta_{\tau_1 \tau_2} \right. \\
& - \sum_k |V_k|^2 \left(\frac{\partial}{\partial \tau_1} + \varepsilon_k \right)^{-1} \delta_{\tau_1 \tau_2} \left. \right] f_\sigma(\tau_2) \\
& + \int_0^\beta d\tau \frac{U}{2} \sum_{\substack{\sigma \sigma' \\ \sigma \neq \sigma'}} \bar{f}_\sigma(\tau) f_\sigma(\tau) \bar{f}_{\sigma'}(\tau) f_{\sigma'}(\tau). \quad (\text{A34})
\end{aligned}$$

If we now compare this to the effective action of the Hubbard model (A23), we see that they are identical if we require that the Weiss function $\mathcal{G}(\tau_1 - \tau_2)$ fulfills the condition

$$\mathcal{G}^{-1}(\tau_1 - \tau_2) = - \left(\frac{\partial}{\partial \tau_1} - \mu \right) \delta_{\tau_1 \tau_2} + \sum_k |V_k|^2 \left(\frac{\partial}{\partial \tau_1} + \varepsilon_k \right)^{-1} \delta_{\tau_1 \tau_2}. \quad (\text{A35})$$

Going from imaginary time to imaginary frequency, this equation reads as

$$\mathcal{G}^{-1}(i\omega_n) = i\omega_n + \mu - \sum_k \frac{|V_k|^2}{i\omega_n - \varepsilon_k}. \quad (\text{A36})$$

Here we can identify the usual definition of the hybridization function $\Delta(i\omega_n)$ in the Anderson impurity model,

$$\Delta(i\omega_n) = \sum_k \frac{|V_k|^2}{i\omega_n - \varepsilon_k}. \quad (\text{A37})$$

If we now equate Weiss functions (A29) and (A36), we find the DMFT self-consistency condition in terms of a prescription for $\Delta(i\omega_n)$:

$$\Delta(i\omega_n) = i\omega_n + \mu - \Sigma_\sigma(i\omega_n) - G_{oo\sigma}^{-1}(i\omega_n). \quad (\text{A38})$$

On the Bethe lattice and with a half bandwidth of $D=2t$, we have a noninteracting density of states,

$$\rho_0(\varepsilon) = \frac{1}{2\pi t^2} \sqrt{4t^2 - \varepsilon^2}, \quad (\text{A39})$$

and thus we can write for the local Green's function (with $\xi = i\omega_n + \mu - \Sigma_\sigma(i\omega_n)$),

$$\begin{aligned}
G_{oo\sigma}(i\omega_n) &= \sum_k G_k(i\omega_n) = \sum_k \frac{1}{\xi - \varepsilon_k} = \int d\varepsilon \frac{\rho_0(\varepsilon)}{\xi - \varepsilon} \\
&= \frac{1}{2\pi t^2} \int_{-2t}^{2t} d\varepsilon \frac{\sqrt{4t^2 - \varepsilon^2}}{\xi - \varepsilon} \\
&= \frac{1}{2t^2} [\xi - \text{sgn}(\text{Re}\xi) \sqrt{\xi^2 - 4t^2}]. \quad (\text{A40})
\end{aligned}$$

From this we gain the expression

$$t^2 G_{oo\sigma}(i\omega_n) - \xi + G_{oo\sigma}^{-1}(i\omega_n) = 0, \quad (\text{A41})$$

which combined with Eq. (A38) leads to a simplified form of the self-consistency condition:

$$\Delta(i\omega_n) = t^2 G_{oo\sigma}(i\omega_n). \quad (\text{A42})$$

APPENDIX B: DMFT SELF-CONSISTENCY CONDITION FOR THE ANDERSON LATTICE

We again focus on one site $i=o$ and split the Hamiltonian into three parts:

$$H_{\text{PAM}} = H_o + H_c + H^{(o)}, \quad (\text{B1})$$

$$\begin{aligned}
H_o = & \varepsilon_c \sum_\sigma c_{o\sigma}^+ c_{o\sigma} + \varepsilon_f \sum_\sigma f_{o\sigma}^+ f_{o\sigma} + \sum_\sigma (V_{o\sigma} c_{o\sigma}^+ f_{o\sigma} + V_{o\sigma}^* f_{o\sigma}^+ c_{o\sigma}) \\
& + \frac{U}{2} \sum_{\substack{\sigma \sigma' \\ \sigma \neq \sigma'}} f_{o\sigma}^+ f_{o\sigma} f_{o\sigma'}^+ f_{o\sigma'}, \quad (\text{B2})
\end{aligned}$$

$$H_c = - \sum_{i\sigma} [t_{io}^c c_{i\sigma}^+ c_{o\sigma} + t_{oi}^c c_{o\sigma}^+ c_{i\sigma}], \quad (\text{B3})$$

$$\begin{aligned}
H^{(o)} = & - \sum_{i \neq o, j \neq o\sigma} t_{ij}^c c_{i\sigma}^+ c_{j\sigma} + \varepsilon_c \sum_{i \neq o\sigma} c_{i\sigma}^+ c_{i\sigma} + \varepsilon_f \sum_{i \neq o\sigma} f_{i\sigma}^+ f_{i\sigma} \\
& + \sum_{i \neq o\sigma} (V_{io} c_{i\sigma}^+ f_{i\sigma} + V_{io}^* f_{i\sigma}^+ c_{i\sigma}) + \frac{U}{2} \sum_{\substack{i \neq o\sigma\sigma' \\ \sigma \neq \sigma'}} f_{i\sigma}^+ f_{i\sigma} f_{i\sigma'}^+ f_{i\sigma'}; \quad (\text{B4})
\end{aligned}$$

H_c has the same form as in the Hubbard model, but the local part H_o is more complicated as it contains two species of electrons, conduction and f electrons. Nevertheless, we can proceed completely along the lines detailed for the Hubbard model above, expanding the action ΔS arising from H_c in order to arrive at an effective action for site o . In this case we have

$$\begin{aligned}
S_o = & \int_0^\beta d\tau \left[\sum_\sigma \bar{f}_\sigma(\tau) \left(\frac{\partial}{\partial \tau} + \varepsilon_f \right) f_\sigma(\tau) \right. \\
& + \frac{U}{2} \sum_{\substack{\sigma \sigma' \\ \sigma \neq \sigma'}} \bar{f}_{o\sigma}(\tau) f_{o\sigma}(\tau) \bar{f}_{o\sigma'}(\tau) f_{o\sigma'}(\tau) \\
& + \sum_\sigma \bar{c}_{o\sigma}(\tau) \left(\frac{\partial}{\partial \tau} + \varepsilon_c \right) c_{o\sigma}(\tau) + \sum_\sigma (V_{o\sigma} \bar{c}_{o\sigma}(\tau) f_{o\sigma}(\tau) \\
& \left. + V_{o\sigma}^* \bar{f}_{o\sigma}(\tau) c_{o\sigma}(\tau)) \right] \quad (\text{B5})
\end{aligned}$$

and

$$S_{\text{eff}} = S_o + \int_0^\beta d\tau_1 \int_0^\beta d\tau_2 \bar{c}_{o\sigma}(\tau_1) c_{o\sigma}(\tau_2) \sum_{ij\sigma} t_{io} t_{oj} G_{ij\sigma}^{(o)}(\tau_1 - \tau_2). \quad (\text{B6})$$

In the $d \rightarrow \infty$ limit, the Green's function becomes

$$G^{-1}(i\omega_n, \mathbf{k}) = \begin{pmatrix} i\omega_n + \mu - \varepsilon_f^0 - \Sigma_f(i\omega_n) & V_k \\ V_k & i\omega_n + \mu - \varepsilon_k \end{pmatrix}. \quad (\text{B7})$$

Inverting the matrix according to

$$M = \begin{pmatrix} A & B \\ B & C \end{pmatrix} \curvearrowright M^{-1} = \frac{1}{\det M} \begin{pmatrix} C & -B \\ -B & A \end{pmatrix}, \quad (\text{B8})$$

we find

$$G(i\omega_n, \mathbf{k}) = \frac{1}{[i\omega_n + \mu - \varepsilon_f^0 - \Sigma_f(i\omega_n)](i\omega_n + \mu - \varepsilon_k) - V_k^2} \times \begin{pmatrix} i\omega_n + \mu - \varepsilon_k & -V_k \\ -V_k & i\omega_n + \mu - \varepsilon_f^0 - \Sigma_f(i\omega_n) \end{pmatrix}. \quad (\text{B9})$$

Thus, we find for the f electron Green's function,

$$G_f(i\omega_n, \mathbf{k}) = \left(i\omega_n + \mu - \varepsilon_f^0 - \Sigma_f(i\omega_n) - \frac{V_k^2}{i\omega_n + \mu - \varepsilon_k} \right)^{-1}, \quad (\text{B10})$$

and for the conduction band Green's function,

$$G_c(i\omega_n, \mathbf{k}) = \left(i\omega_n + \mu - \varepsilon_k - \frac{V_k^2}{i\omega_n + \mu - \varepsilon_f^0 - \Sigma_f(i\omega_n)} \right)^{-1}. \quad (\text{B11})$$

We get the local propagators as $G_f(R=0, i\omega_n) = \sum_{\mathbf{k}} G_f(i\omega_n, \mathbf{k}) e^{ik(R=0)}$ by summation over \mathbf{k} :

$$G_f^{\text{local}}(i\omega_n) = \sum_{\mathbf{k}} G_f(i\omega_n, \mathbf{k}) = \int d\varepsilon \rho_0(\varepsilon) \left(i\omega_n + \mu - \varepsilon_f^0 - \Sigma_f(i\omega_n) - \frac{V(\varepsilon)^2}{i\omega_n + \mu - \varepsilon} \right)^{-1},$$

$$G_c^{\text{local}}(i\omega_n) = \int d\varepsilon \rho_0(\varepsilon) \left(i\omega_n + \mu - \varepsilon - \frac{V(\varepsilon)^2}{i\omega_n + \mu - \varepsilon_f^0 - \Sigma_f(i\omega_n)} \right)^{-1}. \quad (\text{B12})$$

For computational purposes it is useful to note that for the case of an energy independent $V(\varepsilon) \equiv V$, $G_c^{\text{local}}(i\omega_n)$ can be written as a Hilbert transform $\tilde{D}(\zeta) = \int_{-\infty}^{\infty} d\varepsilon D(\varepsilon) / (\zeta - \varepsilon)$:

$$G_c^{\text{local}}(i\omega_n) = \tilde{D} \left(i\omega_n + \mu - \frac{V^2}{i\omega_n + \mu - \varepsilon_f^0 - \Sigma_f(i\omega_n)} \right). \quad (\text{B13})$$

Rewriting $G_f^{\text{local}}(i\omega_n)$, we can likewise reduce the energy integral to the calculation of a Hilbert transform:

$$G_f^{\text{local}}(i\omega_n) = \int d\varepsilon \rho_0(\varepsilon) \left\{ \frac{1}{i\omega_n + \mu - \varepsilon_f^0 - \Sigma_f(i\omega_n)} + \frac{V^2}{[i\omega_n + \mu - \varepsilon_f^0 - \Sigma_f(i\omega_n)]^2} \times \frac{1}{i\omega_n + \mu - \varepsilon - \frac{V^2}{i\omega_n + \mu - \varepsilon_f^0 - \Sigma_f(i\omega_n)}} \right\}, \quad (\text{B14})$$

and with Eq. (B13),

$$G_f^{\text{local}}(i\omega_n) = \frac{1}{i\omega_n + \mu - \varepsilon_f^0 - \Sigma_f(i\omega_n)} + \frac{V^2}{[i\omega_n + \mu - \varepsilon_f^0 - \Sigma_f(i\omega_n)]^2} G_c^{\text{local}}(i\omega_n). \quad (\text{B15})$$

If we now assume a semicircular DOS $D(\varepsilon) = (1/2\pi t^2) \sqrt{4t^2 - \varepsilon^2}$ for the hybridization V_k we can explicitly write for the Hilbert transform,

$$\tilde{D}(\zeta) = \frac{1}{2\pi t^2} \int_{-2t}^{2t} d\varepsilon \frac{\sqrt{4t^2 - \varepsilon^2}}{\zeta - \varepsilon} = \frac{1}{2t^2} [\zeta - \text{sgn}(\text{Re}\zeta) \sqrt{\zeta^2 - 4t^2}]. \quad (\text{B16})$$

Thus, on the Bethe lattice the self-consistency condition can be calculated without an integral over energies. We also need the Dyson equation,

$$G_0^{-1}(i\omega_n) = G_f^{-1}(i\omega_n) + \Sigma(i\omega_n). \quad (\text{B17})$$

From the high frequency limit of this equation we can find the form of the Weiss function $\mathcal{G}_0^{-1}(i\omega_n)$ by comparing the terms of the expansion order by order. Expanding Eq. (B12) we find

$$G_f(i\omega_n) \approx \frac{1}{i\omega_n} + [\varepsilon_f^0 - \mu + \Sigma_f(i\omega_n)] \left(\frac{1}{i\omega_n} \right)^2 \quad \text{for } i\omega_n \rightarrow \infty. \quad (\text{B18})$$

Expanding the inverse, we find

$$G_f^{-1}(i\omega_n) \approx i\omega_n + \mu - \varepsilon_f^0 - \Sigma_f(i\omega_n) \quad \text{for } i\omega_n \rightarrow \infty. \quad (\text{B19})$$

Thus, we find from Eq. (B17) the high frequency form of the Weiss function:

$$\mathcal{G}_0^{-1}(i\omega_n) \approx i\omega_n + \mu - \varepsilon_f^0. \quad (\text{B20})$$

The hybridization function $\Delta(i\omega_n)$ contains what we have neglected in the high frequency expansion:

$$G_0^{-1}(i\omega_n) = i\omega_n + \mu - \varepsilon_f^0 - \Delta(i\omega_n). \quad (\text{B21})$$

*Electronic address: jeschke@physics.rutgers.edu

†Electronic address: kotliar@physics.rutgers.edu

- ¹For a review, see A. Georges, G. Kotliar, W. Krauth, and M. J. Rozenberg, *Rev. Mod. Phys.* **68**, 13 (1996), and references therein.
- ²W. Metzner and D. Vollhardt, *Phys. Rev. Lett.* **62**, 324 (1989).
- ³A. Georges and G. Kotliar, *Phys. Rev. B* **45**, 6479 (1992).
- ⁴E. Müller-Hartmann, *Z. Phys. B: Condens. Matter* **74**, 507 (1989).
- ⁵V. Anisimov, A. Poteryaev, M. Korotin, A. Anokhin, and G. Kotliar, *J. Phys.: Condens. Matter* **9**, 7359 (1997).
- ⁶S. Y. Savrasov, G. Kotliar, and E. Abrahams, *Nature (London)* **410**, 793 (2001).
- ⁷K. Held, A. K. McMahan, and R. T. Scalettar, *Phys. Rev. Lett.* **87**, 276404 (2001).
- ⁸For a review, see K. Held, I. A. Nekrasov, G. Keller, V. Eyert, N. Blümer, A. K. McMahan, R. T. Scalettar, Th. Pruschke, V. I. Anisimov, and D. Vollhardt, *Psi-k Newsletter #56*, 2003, p. 65; and A. I. Lichtenstein, M. I. Katsnelson, and G. Kotliar, in *Electron Correlations and Materials Properties 2*, edited by A. Conis *et al.* (Kluwer Academic/Plenum Publishers, New York, 2003), p. 75.
- ⁹J. E. Hirsch and R. M. Fye, *Phys. Rev. Lett.* **56**, 2521 (1986).
- ¹⁰H. Keiter and J. C. Kimball, *Int. J. Magn.* **1**, 233 (1971).
- ¹¹H. Kajueter and G. Kotliar, *Phys. Rev. Lett.* **77**, 131 (1996).
- ¹²A. Theumann, *Phys. Rev.* **178**, 978 (1969).
- ¹³C. Lacroix, *J. Phys. F: Met. Phys.* **11**, 2389 (1981).
- ¹⁴Y. Meir, N. S. Wingreen, and P. A. Lee, *Phys. Rev. Lett.* **70**, 2601 (1993).
- ¹⁵T. A. Costi, *J. Phys. C* **19**, 5665 (1986).
- ¹⁶F. D. M. Haldane, *Phys. Rev. Lett.* **40**, 416 (1978).
- ¹⁷H. G. Luo, J. J. Ying, and S. J. Wang, *Phys. Rev. B* **59**, 9710 (1999).
- ¹⁸C. Gros, *Phys. Rev. B* **50**, 7295 (1994).
- ¹⁹A. Georges, G. Kotliar, and W. Krauth, *Z. Phys. B: Condens. Matter* **92**, 313 (1993).
- ²⁰J. Zaanen, G. A. Sawatzky, and J. W. Allen, *Phys. Rev. Lett.* **55**, 418 (1985).